Electronic Supplementary Information

Single-phase gadolinium-doped ceria cathode for highly efficient CO_2 electrolysis

Ahmad Shaur, Michel Drazkowski, Shaochen Zhu, Bernard Boukamp and Henny J.M. Bouwmeester

---

Ahmad Shaur, Michel Drazkowski, Shaochen Zhu, Henny J.M. Bouwmeester
Electrochemistry Research Group, MESA+ Institute for Nanotechnology, University of Twente, P.O. Box 217, 7500 AE, Enschede, The Netherlands
E-mail: h.j.m.bouwmeester@utwente.nl

Bernard Boukamp
Inorganic Materials Science Group, MESA+ Institute for Nanotechnology, University of Twente, P.O. Box 217, 7500 AE, Enschede, The Netherlands

Henny J.M. Bouwmeester
CAS Key Laboratory of Materials for Energy Conversion, Department of Materials Science and Engineering, University of Science and Technology of China, Hefei, 230026, P. R. China

Henny J.M. Bouwmeester
Forschungszentrum Jülich GmbH, Institute of Energy and Climate Research-IEK-1, Leo- Brandt-Str. 1, D-52425, Jülich, Germany

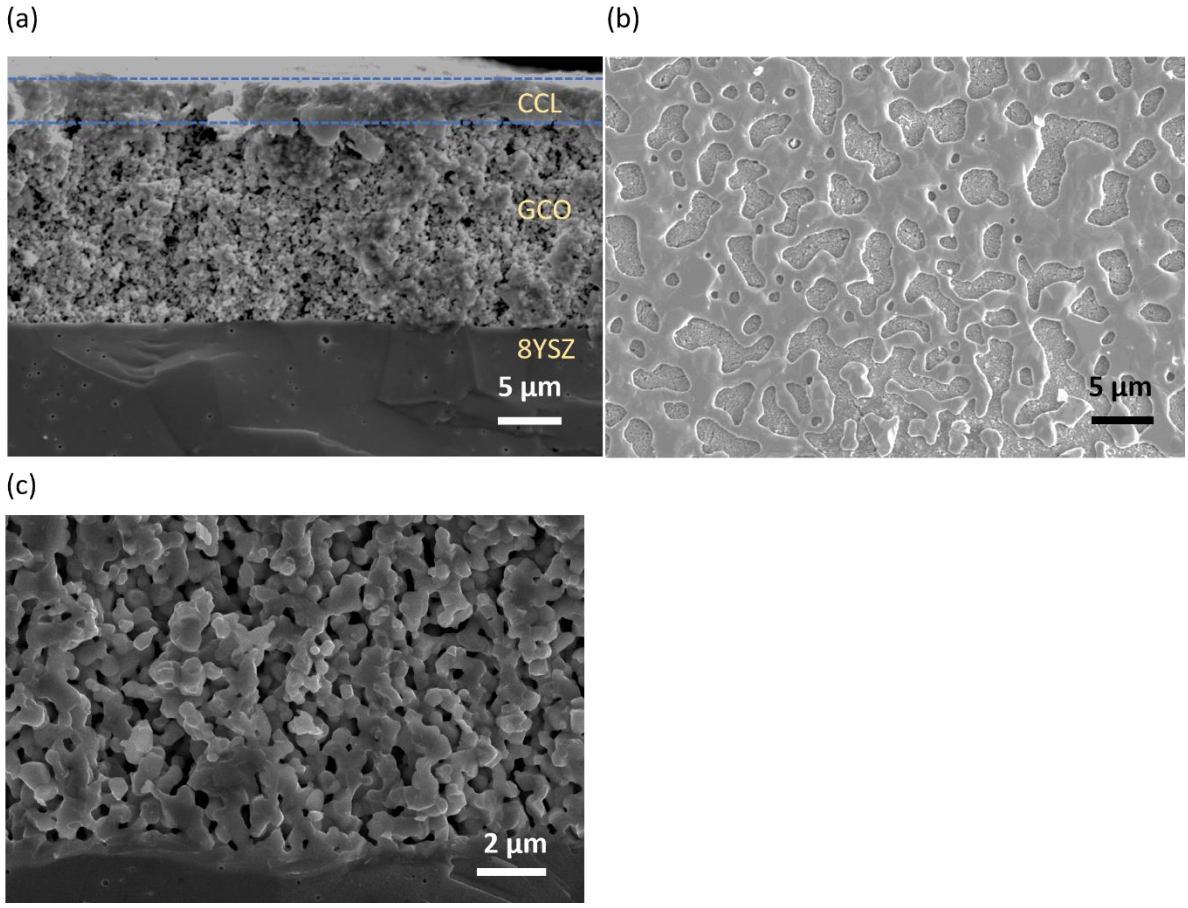

Fig. S1 SEM images of a) cross-sectional view of the GCO/8YSZ-electrolyte interface, b) top view of the gold current collecting layer (CCL), and c) post-mortem analysis of the electrolyte-electrode interface.

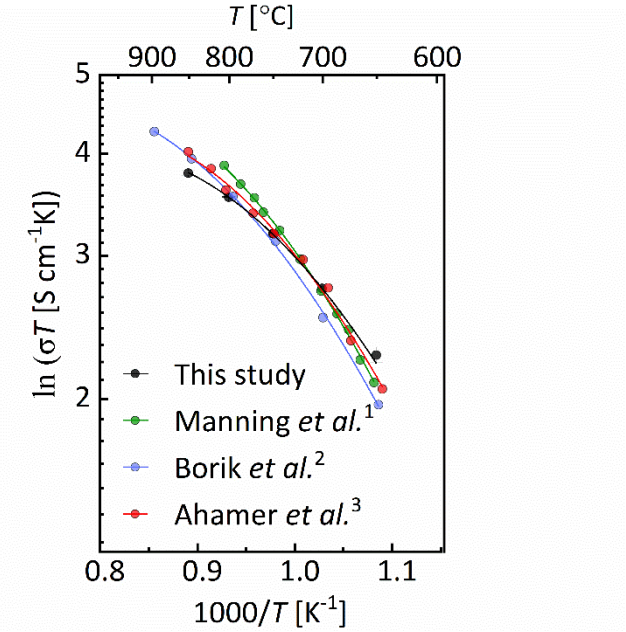

Fig. S2 Arrhenius plot of the ionic conductivity of 8 mol% yttria-stabilized zirconia (8YSZ) calculated from data of $R_{\mathrm{el/te}}$ (Table S4) with data reported in literature.[1-3]

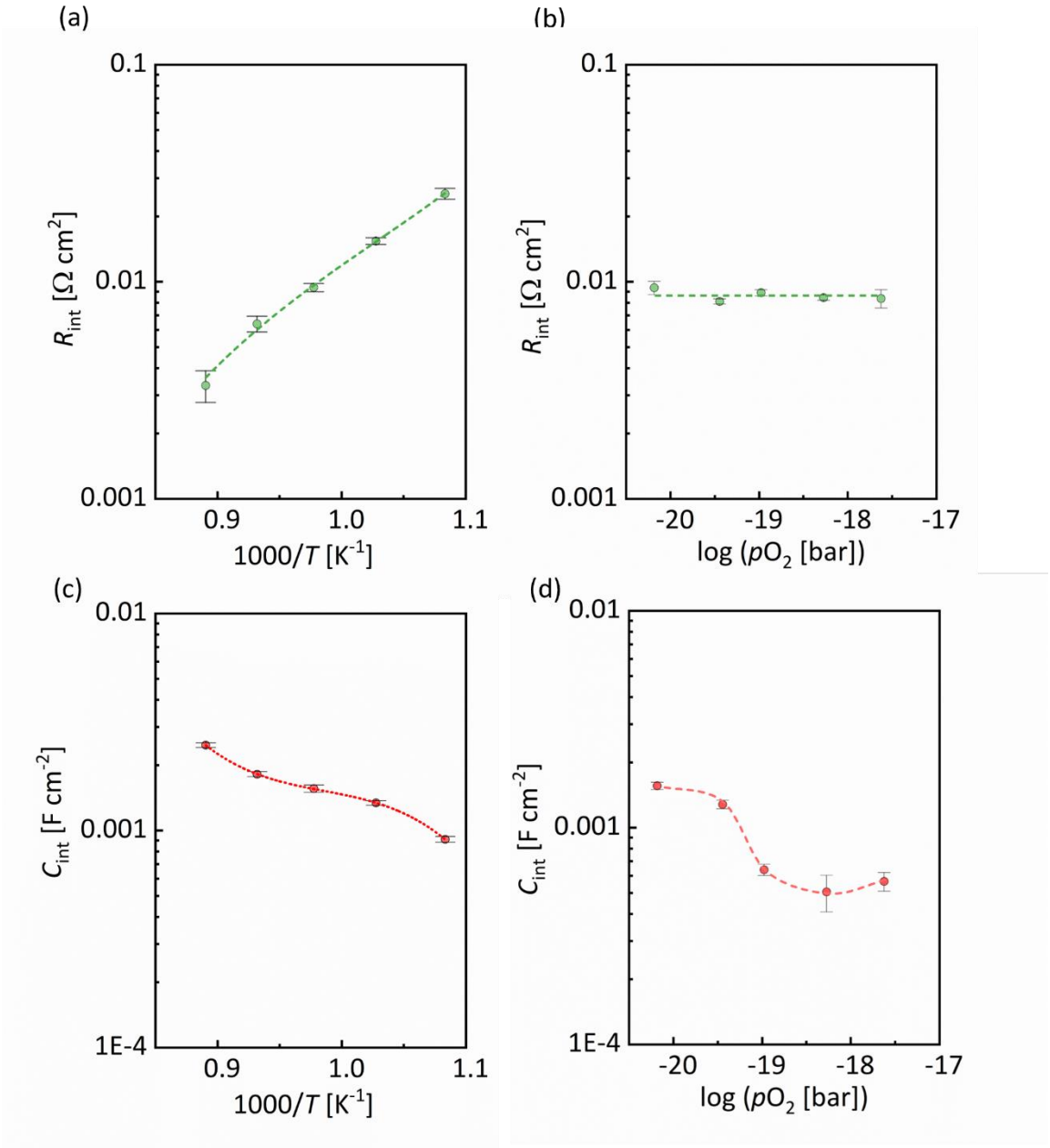

Fig. S3 Arrhenius plot and oxygen partial pressure dependence of (a, b), ion transfer resistance (R_{int}) and (c, d) effective capacitance (C_{int}). Data obtained from equivalent circuit fitting of impedance spectra of symmetrical cells, GCO | 8YSZ | GCO, recorded (a, c) at different temperatures in CO_2/CO 50/50 and (b, d) at 750 °C in different CO_2/CO gas mixtures.

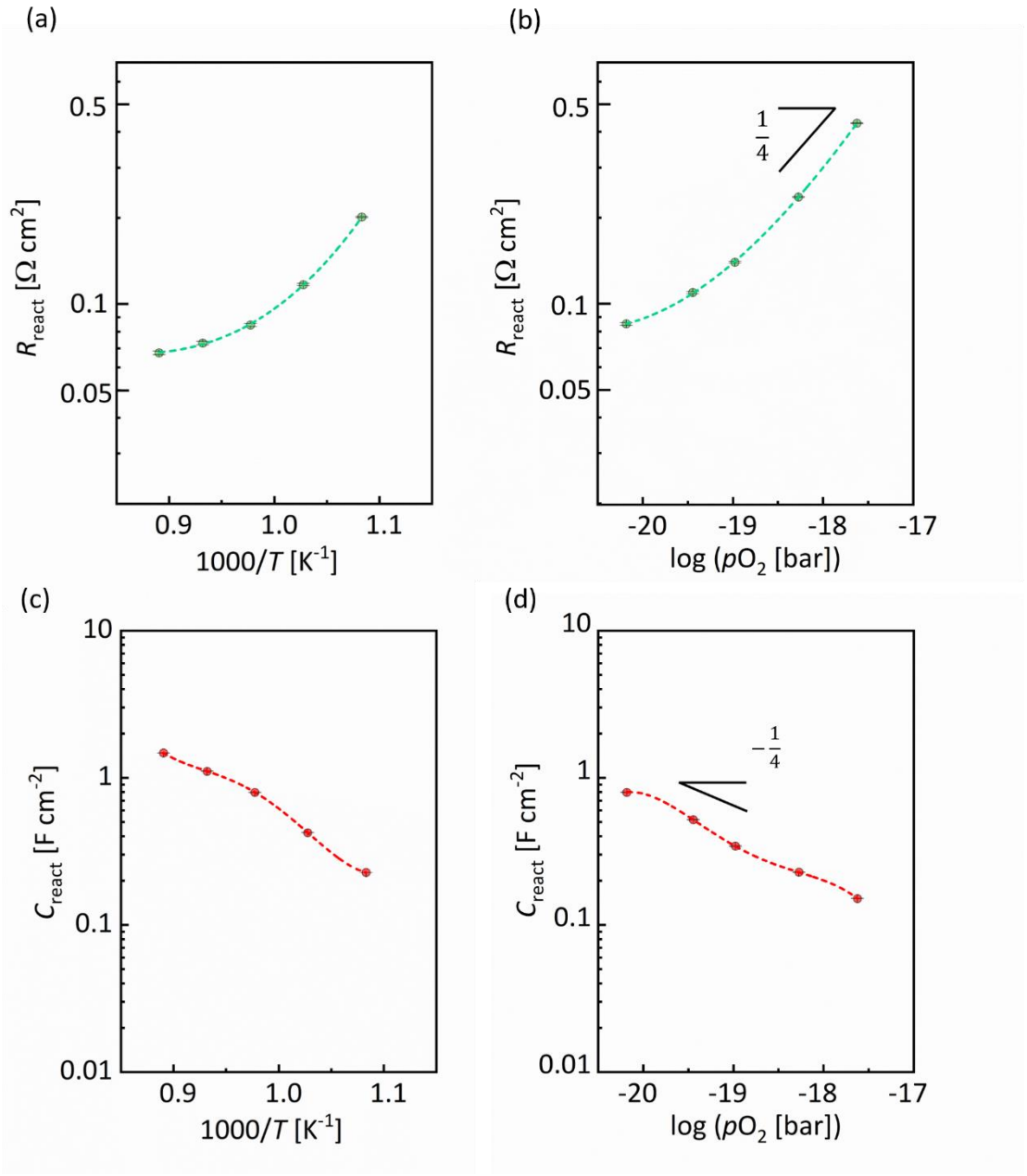

Fig. S4 Arrhenius plot and oxygen partial pressure dependence of (a, b) surface reaction resistance (R_{react}) and (c, d) effective capacitance (C_{react}). Data obtained from equivalent circuit fitting of impedance spectra of symmetrical cells, GCO | 8YSZ | GCO, recorded (a, c) at different temperatures in CO_2/CO 50/50 and (b, d) at 750 °C in different CO_2/CO gas mixtures. The dashed lines serve as guides for the eye.

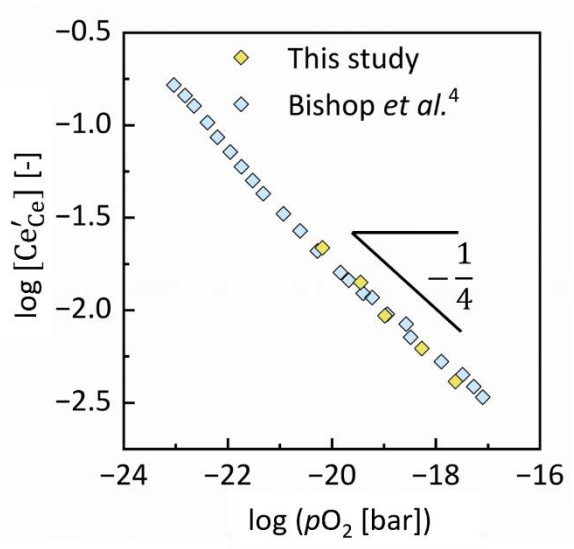

Fig. S5 Comparison of electron carrier concentrations $[\mathrm{Ce}'_{\mathrm{Ce}}]$ at 750 °C determined from the oxygen partial pressure-dependent capacitance data (shown in Fig. S4c) using eqn (2) with corresponding values calculated from data of oxygen non-stoichiometry of GCO reported by Bishop *et al.*[1]

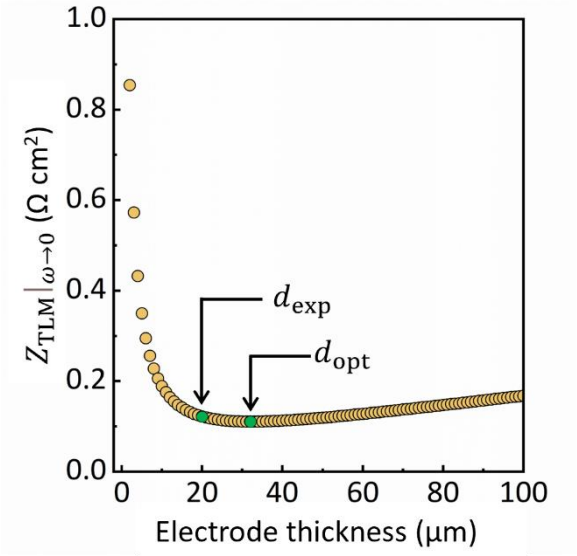

Fig. S6 $Z_{\mathrm{TLM}}|_{\omega\to 0}$ as a function of GCO electrode thickness, showing an optimal electrode thickness (d_{opt}) at around 32 µm. Values of $Z_{\mathrm{TLM}}|_{\omega\to 0}$ were calculated after thickness-dependent scaling of the resistance values R_{ion}, R_{eon} and R_{react} determined at 750 °C in CO_2/CO 50/50 (listed in Table S3). The parameter d_{exp} represents the experimentally applied electrode thickness.

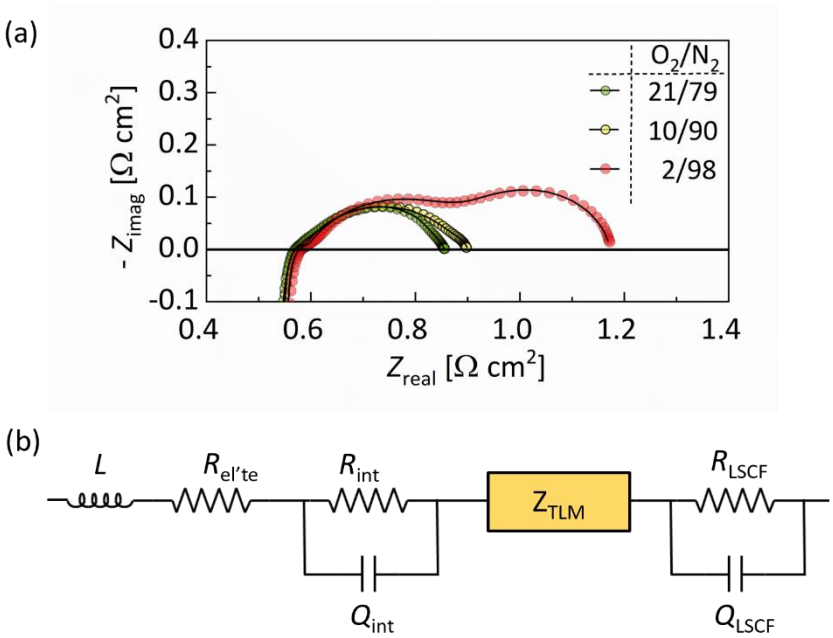

Fig. S7 a) Impedance spectra of the full cell (O_2/N_2) LSCF | GCO | 8YSZ | GCO (CO_2/CO 90/10) recorded at 750 °C under OCV in different O_2/N_2 gas mixtures, and b) equivalent circuit used for fitting. Corresponding data obtained from fitting are listed in Table S6.

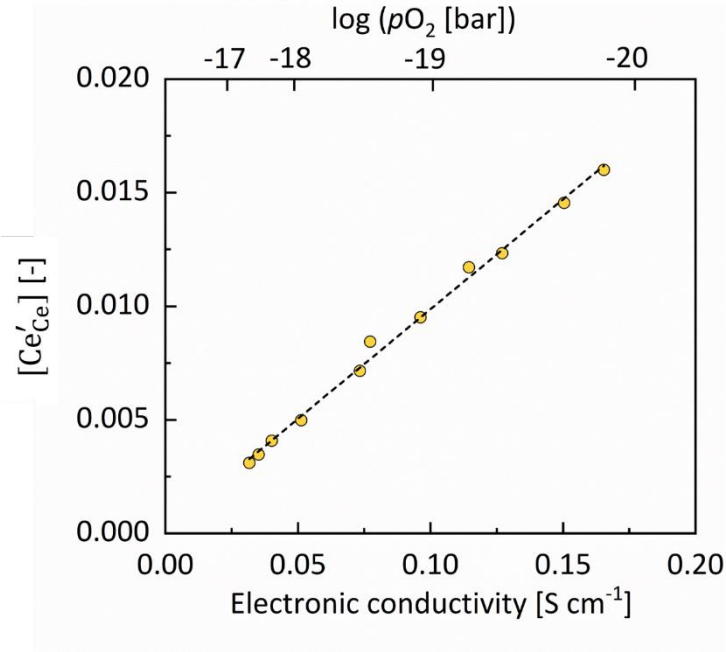

Fig. S8 Correlation between electron carrier concentration $[\mathrm{Ce}'_{\mathrm{Ce}}]$ and electronic conductivity at 750 °C. Data of $[\mathrm{Ce}'_{\mathrm{Ce}}]$ were calculated from oxygen non-stoichiometry data of GCO reported by Bishop *et al*.[4] The electronic conductivity of GCO is calculated using $\sigma_{\mathrm{eon}} = \sigma^0_{\mathrm{eon}} {pO_2}^m$. Values of σ^0_{eon} and m obtained from fitting experimental data of the total conductivity (Fig. 6) are listed in Table S5. The linear relationship between both parameters reflects a constant mobility of the electronic charge carriers within the experimental range. The dashed straight line is from linear regression analysis of the data.

Table S1. Electrode parameters and equations for estimating values of R_{ion} and R_{eon} used for fitting of data of impedance spectroscopy. Conductivity and resistance values are specified for 750 °C.

Parameter	Value	Reference/equation
Thickness (l)	20 µm	Estimate from SEM cross-sections
Geometrical surface area (A)	0.785 cm^2	
Porosity (ϵ)	0.37	Estimate from SEM cross-sections
Tortuosity (τ)	1.5	Ref. [2]
Ionic conductivity (σ_{ion})	0.055 S cm^{-1}	Fig. 6
Effective ionic conductivity ($\sigma_{\mathrm{ion,eff}}$)	0.023 S cm^{-1}	$\sigma_{\mathrm{ion,eff}} = \frac{\sigma_{\mathrm{ion}}(1-\varepsilon)}{\tau}$
Effective ionic resistance (R_{ion})	0.086 Ω cm^2	$R_{\mathrm{ion}} = \frac{l}{\sigma_{\mathrm{ion,eff}}}$
Electronic conductivity (σ_{eon})	0.17 S cm^{-1}	Fig. 6 ($pO_2 \approx 10^{-20.1}$ bar)
Effective electronic conductivity ($\sigma_{\mathrm{eon,eff}}$)	0.070 S cm^{-1}	$\sigma_{\mathrm{eon,eff}} = \frac{\sigma_{\mathrm{eon}}(1-\epsilon)}{\tau}$ ($pO_2 \approx 10^{-20.1}$ bar)
Effective electronic resistance (R_{eon})	0.028 Ω cm^2	$R_{\mathrm{eon}} = \frac{l}{\sigma_{\mathrm{eon,eff}}}$ ($pO_2 \approx 10^{-20.1}$ bar)

Table S2. Best-fit parameters obtained from equivalent circuit fitting of the impedance spectrum shown in Fig. 3a.

Parameter	Value	Unit	Error	Error%
L	377.8 x 10^{-9}	H	0.8 x 10^{-9}	0.2
$R_{\mathrm{el/te}}$	0.488	Ω cm^2	0.001	0.2
R_{int}	9.2 x 10^{-3}	Ω cm^2	0.9 x 10^{-3}	9.5
Q_{int}	9.2 x 10^{-3}	$\mathrm{F\ s^{\alpha_{int}-1}\ cm^{-2}}$	1.6 x 10^{-3}	17.3
α_{int}	0.87	-	0.025	2.8
R_{eon}	0.023	Ω cm^2	0.001	4.2
R_{ion}	0.072	Ω cm^2	0.002	2.0
R_{react}	0.085	Ω cm^2	0.001	0.5
Q_{react}	1.120	$\mathrm{F\ s^{\alpha_{react}-1}\ cm^{-2}}$	0.004	0.5
α_{react}	0.809	-	0.002	0.3
Goodness of fit: χ^2 = 4.8 x 10^{-7}				

Table S3. Resistance values obtained from fitting impedance spectra of symmetrical cells GCO | 8YSZ | GCO recorded at 750 °C in different CO_2/CO gas mixtures.

CO_2/CO	R_{∞} (Ω cm^2)	$R_{\mathrm{el/te}}$ (Ω cm^2)	R_{int} (Ω cm^2)	R_{eon} (Ω cm^2)	R_{ion} (Ω cm^2)	R_{p} (Ω cm^2)	R_{react} (Ω cm^2)	ASR (Ω cm^2)
50/50	0.525 ± 0.001	0.488 ± 0.002	0.009 ± 0.001	0.028	0.086	0.021	0.085 ± 0.001	0.131 ± 0.001
70/30	0.549 ± 0.001	0.489 ± 0.003	0.009 ± 0.001	0.078	0.086	0.041	0.109 ± 0.001	0.172 ± 0.001
80/20	0.557 ± 0.001	0.478 ± 0.002	0.009 ± 0.001	0.118	0.086	0.049	0.141 ± 0.001	0.217 ± 0.001
90/10	0.580 ± 0.001	0.475 ± 0.001	0.008 ± 0.002	0.216	0.086	0.061	0.234 ± 0.001	0.341 ± 0.001
95/05	0.607 ± 0.001	0.478 ± 0.005	0.009 ± 0.002	0.379	0.086	0.070	0.427 ± 0.003	0.586 ± 0.002

Table S4. Resistance values obtained from fitting impedance spectra of symmetrical cells GCO | 8YSZ | GCO recorded at different temperatures in CO_2/CO 50/50.

T (°C)	R_{∞} (Ω cm^2)	$R_{\mathrm{el/te}}$ (Ω cm^2)	R_{int} (Ω cm^2)	R_{eon} (Ω cm^2)	R_{ion} (Ω cm^2)	R_{p} (Ω cm^2)	R_{react} (Ω cm^2)	ASR (Ω cm^2)
650	1.168 ± 0.006	1.047 ± 0.020	0.026 ± 0.001	0.110	0.173	0.061	0.202 ± 0.001	0.320 ± 0.006
700	0.792 ± 0.005	0.742 ± 0.001	0.015 ± 0.001	0.044	0.127	0.031	0.117 ± 0.001	0.187 ± 0.002
750	0.525 ± 0.001	0.488 ± 0.002	0.009 ± 0.001	0.023	0.086	0.018	0.085 ± 0.001	0.131 ± 0.001
800	0.395 ± 0.001	0.387 ± 0.001	0.006 ± 0.001	0.004	0.051	0.004	0.073 ± 0.001	0.096 ± 0.001
850	0.327 ± 0.001	0.323 ± 0.002	0.003 ± 0.001	0.002	0.034	0.002	0.067 ± 0.001	0.081 ± 0.001

Table S5. Parameters obtained from fitting experimental data of the total conductivity (Fig. 6) to $\sigma_{\mathrm{tot}} = \sigma_{\mathrm{ion}} + \sigma_{\mathrm{eon}}^{0} \times {pO_2}^{m}$.

T (°C)	σ_{ion} (S cm^{-1})	$\sigma_{\mathrm{eon}}^{0}$ (S cm^{-1})	*m* (-)
650	0.028	6.31 x 10^{-8} ± 3 x 10^{-10}	-0.249 ± 0.008
700	0.039	2.72 x 10^{-7} ± 7 x 10^{-10}	-0.260 ± 0.008
750	0.055	1.00 x 10^{-6} ± 1 x 10^{-8}	-0.265 ± 0.002
800	0.076	3.30 x 10^{-6} ± 3 x 10^{-8}	-0.279 ± 0.003
850	0.113	8.07 x 10^{-6} ± 3 x 10^{-7}	-0.291 ± 0.011

Table S6. Resistance values obtained from fitting impedance spectra of full cells (O_2/N_2) LSCF | GCO | 8YSZ | GCO (CO_2/CO 90/10) recorded at 750 °C under OCV in different O_2/N_2 gas mixtures.

pO_2 (atm)	R_∞ (Ω cm^2)	$R_{\mathrm{el/te}}$ (Ω cm^2)	R_{int} (Ω cm^2)	R_{eon} (Ω cm^2)	R_{ion} (Ω cm^2)	R_{p} (Ω cm^2)	R_{react} (Ω cm^2)	R_{LSCF} (Ω cm^2)	R_{pol} (Ω cm^2)
0.21	0.569 ± 0.001	0.517 ± 0.001	0.032± 0.009	0.216	0.086	0.061	0.266 ± 0.003	0.006 ± 0.001	0.352 ± 0.001
0.10	0.572 ± 0.001	0.520 ± 0.001	0.024 ± 0.008	0.216	0.086	0.061	0.262 ± 0.010	0.040 ± 0.001	0.378 ± 0.016
0.02	0.576 ± 0.006	0.524 ± 0.001	0.025 ± 0.008	0.216	0.086	0.061	0.277 ± 0.012	0.212 ± 0.003	0.521 ± 0.043

References

1 P. Manning, J. Sirman, R. De Souza and J. Kilner, *Solid State Ionics,* 1997, **100**, 1-10.

2 M. A. Borik, S. I. Bredikhin, V. T. Bublik, A. V. Kulebyakin, I. E. Kuritsyna, E. E. Lomonova, P. O. Milovich, V. A. Myzina, V. V. Osiko, P. A. Ryabochkina and N. Y. Tabachkova, *J. Am. Ceram.*, 2017, **100**, 5536-5547.

3 C. Ahamer, A. K. Opitz, G. M. Rupp and J. Fleig, *J. Electrochem. Soc.*, 2017, **164**, F790-F803.

4 S. R. Bishop, K. L. Duncan and E. D. Wachsman, *Acta Materialia*, 2009, **57**, 3596-3605.

5 A. Nenning, M. Holzmann, J. Fleig and A. K. Opitz, *Materials Adv.*, 2021, **2**, 5422-5431.